
Scalable Computing: Practice and Experience, ISSN 1895-1767, http://www.scpe.org
© 2024 SCPE. Volume 25, Issues 5, pp. 3523–3530, DOI 10.12694/scpe.v25i5.3071

HIGH-RESOLUTION HOLOGRAPHIC IMAGE RECONSTRUCTION BASED ON DEEP LEARNING

FANGJU LI*

Abstract. Aiming at the shortcomings of existing holographic reconstruction algorithms, which are complex and easily affected by noise, this project proposes a semantic partitioning U-Net for high-resolution reconstruction. Firstly, a method based on the edge-neural network is proposed to obtain more image semantic information and improve the model training effect. Secondly, the effective channel attention mechanism of deep neural networks is introduced to enhance the attention to the detailed information in the holographic image. This further improves the accuracy of the neural network. The convergence rate of the neural network is accelerated by introducing a linear element with leakage correction. Experimental results show that this method can quickly reconstruct phase and brightness images with better detail, better edge texture and flat background. Holographic images of various sizes can be reproduced. The research of this project will lay a foundation for applying holographic image enhancement technology based on deep learning.

Key words: Holography; High-resolution reconstruction; Channel attention mechanism; Terminal neural network; multi-scale reconstruction

1. Introduction. The numerical reconstruction of holograms is a very crucial research work. Firstly, it needs to transform the hologram, filter it +1 times, carry out operations such as unwrapping and phase compensation, and finally realize the reconstruction of the hologram. However, conventional detection technology is more complicated and easily disturbed by noise. So, it is necessary to find a fast and effective reconstruction algorithm. In recent years, with the rapid development of neural networks and corresponding algorithms, it has played a vital role in many industries such as industry, agriculture, medicine and so on with its convenient, fast and efficient characteristics, and it also dramatically promotes the development of three-dimensional image reconstruction. It is imperative to construct an end-to-end coaxial holographic reconstruction network that can resist various optical path aberrations and has no restriction on the wavefront of the reference beam. High-resolution holographic image reconstruction with deep learning is based on deep neural networks, which can reconstruct low-resolution holographic images into high-resolution images. This method takes advantage of the powerful capabilities of convolutional neural networks (CNN) and recurrent neural networks (RNN) in deep learning to learn the features and structure of images, thereby achieving the reconstruction of high-resolution holographic images. Specifically, this approach typically includes the following steps:

1. Data preprocessing: Convert the original low-resolution holographic image into a format suitable for input into the deep learning model and perform necessary preprocessing, such as denoising, normalization, etc.
2. Feature extraction: Use the convolutional neural network (CNN) in the deep learning model to extract features from the preprocessed holographic image to extract high-level features of the image.
3. Super-resolution reconstruction: Use the deep learning model's recurrent neural network (RNN) to perform super-resolution reconstruction on the extracted high-level features to generate high-resolution holographic images.
4. Post-processing: Perform necessary post-processing on the generated high-resolution holographic image, such as denoising, sharpening, etc., to improve the quality and visibility of the image. The high-resolution holographic image reconstruction method of deep learning is a complex technology that requires a large amount of computing resources and training data. It also requires understanding and mastery of deep

*Department of Physics, School of Physics and Electrical Engineering, Weinan Normal University, Weinan, Shaanxi, 714099, China (anty8366@163.com)

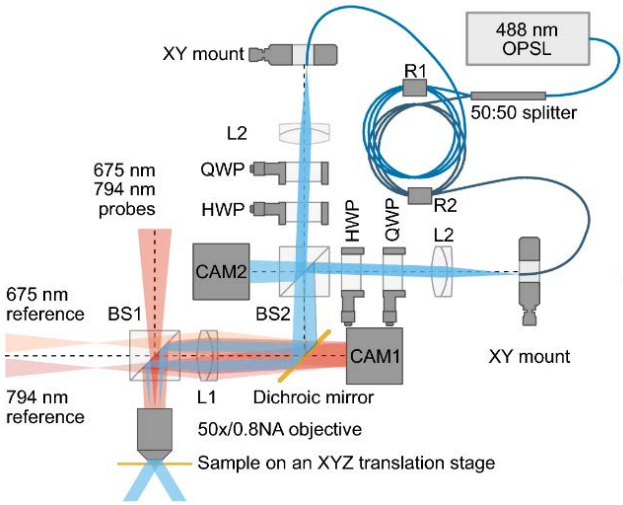

Fig. 2.1: *Principle of digital holographic recording.*

learning models and algorithms.

Reference [1] describes a lightweight one-to-two network, which can reproduce both light intensity and bit phase and is applied to digital image reconstruction. In literature [2], U-shaped networks were used to reconstruct three-dimensional images, and the images were not affected by DC, twins and other factors. Reference [3] introduced the attention mechanism into U-Net to achieve high-resolution cell reconstruction. In reference [4], a multi-scale complete convolutional fusion network was constructed to reconstruct the three-dimensional phase diagram of a single cell. Literature has some problems [5], such as low reconstruction rate, complex reconstructed scenes and unclear boundaries. The existing studies only conducted simulation experiments, lacking the real image test. This project will combine the end-to-end neural network with adequate channel attention (ECA) based on U-Net architecture to improve reconstruction efficiency. This project proposes an end-to-end neural network model based on U-Net to improve reconstruction efficiency further. Adequate channel attention is introduced into the feature extraction layer. The method of leakage correction was used to improve the linear cell activation function of the convolutional hidden layer. Then, an efficient and high-quality reconstruction method of multi-scale hologram images based on skeleton structure is proposed.

2. Principles and methods.

2.1. Digital holographic wavefront recording and traditional reconstruction. The reference light is coherently superimposed utilizing object-light wave transmission on the hologram. The interference fringe pattern collected by CCD and a digital hologram are obtained. The principle of digital holographic recording is shown in Figure 2.1 (the picture is quoted in the literature [6]).

Assuming that the density of the object surface is $P(u_0, v_0)$, the complex amplitude of the object wave reaching the holographic recording surface after coherent light irradiation is obtained by the method of angular spectral diffraction.

$$P(u,v) = G^{-1}\left\{G\left[P\left(u_0,v_0\right)\right]\exp\left[k\frac{2\pi}{\eta}s\sqrt{1-\left(\eta g_{x_0}\right)^2-\left(\eta g_{y_0}\right)^2}\right]\right\}$$

G is the Fourier transform. G^{-1} inverse Fourier inversion. s is the distance from the surface of the object to the projection plane of the hologram. $P(u,v) = C(u,v)\exp[k\eta(u,v)]$. It is assumed that $C(u,v)$ represents the light wave amplitude of the object and $\eta(u,v)$ represents the phase of the light wave of the object [7]. The complex amplitude of the reference light on the hologram is called $D(u,v) = C_d(u,v)\exp\left[k\eta_d(u,v)\right]$. Where $C_d(u,v)$

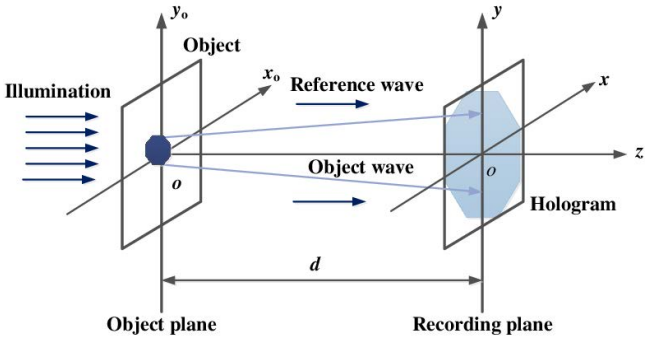

Fig. 2.2: *Schematic diagram of digital holographic reconstruction.*

represents the amplitude of the reference light wave and $\eta_d(u,v)$ represents the phase. Then, the distribution of light intensity on the recording surface of digital holography can be expressed as:

$$W(u,v) = |P(u,v) + D(u,v)|^2 = \\ |P(u,v)|^2 + |D(u,v)|^2 + \\ P(u,v)D^*(u,v) + P^*(u,v)D(u,v)$$

$|P(u,v)|^2$ represents information about the light intensity of the object and $|D(u,v)|^2$ represents information about the intensity of the reference light. The third project is to use conjugated light to regulate matter waves. The fourth project is the study of conjugated optical properties of reference light sources [8]. Therefore, the measured object's amplitude and bit equality information are recorded in the digital hologram. The reproduction principle of traditional digital holography is shown in Figure 2.2. The reconstruction of the image is realized through the steps of illumination and zero-order interference, twin image elimination and phase unwinding using regenerative light. The above processes are not included in reconstructing digital holograms using deep neural networks, so they will not be described here.

Assuming that the copied light wave is A vertically irradiated plane wave $H(u,v)$, then after irradiated digital holography, the diffraction wave generated can be expressed as:

$$W'(u,v) = H(u,v)W(u,v) = H(u,v)\left[|D(u,v)|^2 + |P(u,v)|^2\right] + \\ H(u,v)D^*(u,v)P(u,v) + H(u,v)D(u,v)P^*(u,v)$$

From the diffraction equation of the angular spectrum, the light field of the reproducing object can be obtained:

$$P(u_i,v_i) = G^{-1}\left\{G\left[W'(u,v)\right]\exp\left[k\frac{2\pi}{\eta}s\sqrt{1-(\eta g_u)^2-(\eta g_v)^2}\right]\right\}$$

2.2. Neural network structure. The experiment was divided into two parts. The network structure used in the first experiment is shown in Figure 2.3. Where $U\times Q$ is the proportion of the input image. $U/2\times Q/2$ represents that the digital holographic image on the $U\times Q$ scale is $1/2$ of the original scale after being maximized. The rectangular frame is the characteristic graph obtained after processing each operation module [9]. The number of channels on the current feature map is displayed above the rectangular box. Here, the input and output represented by 1 are two gray images. $Z1$ means that the number of channels in the current characteristic mapping is not fixed and is given according to specific test requirements. $2Z1, 4Z1$, etc., represent the current number of characteristic graph channels is 2 times, 4 times, and $Z1$ so on. The network architecture comprises five operation modules: hierarchical segmentation block, down sampling block, up sampling block, jump link block, output convolutional layer and so on. See Figure 2.3 for a detailed description of each module.

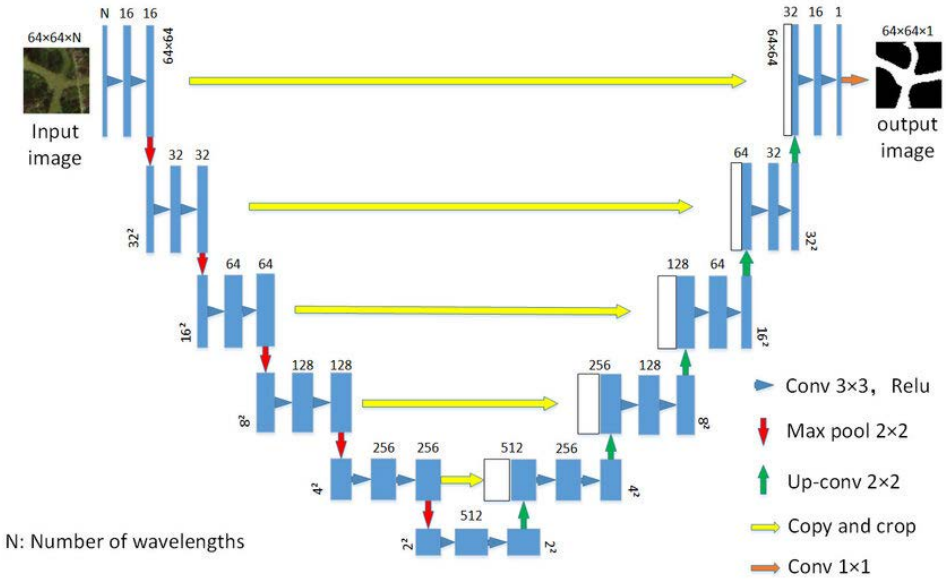

Fig. 2.3: *Improved U-Net structure.*

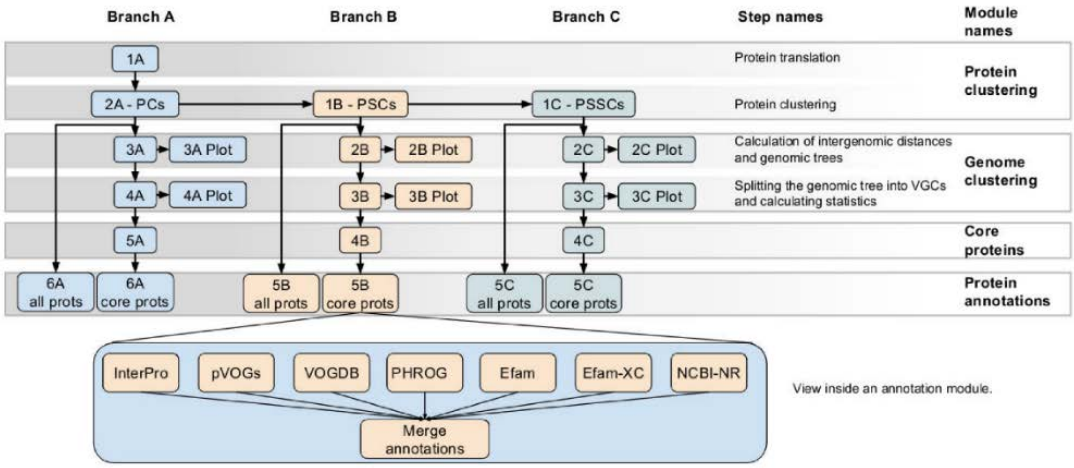

Fig. 2.4: *HS-Block structure.*

2.2.1. Dividing blocks by layers. This construct is shown in Figure 2.4. The core idea is to use a 3x3 convolution kernel to extract the feature map, perform Batch Norm and ReLU operations, and divide it into five channels. The output of the first set is fed directly to the next level. The second set of images is also extracted by a 3x3 convolutional network with a convolution kernel, and these images are evenly divided into two sub-sequences [10]. The first sub-sequence is connected with the second sub-sequence, and finally, the depth features are further extracted by convolution and the average segmentation is carried out until the fifth set of images is completed. Finally, the output characteristic diagram is integrated and used as the input of the next layer. The advantage of this method is that it reduces the redundant features based on reducing the network structure and improves the operational efficiency and speed of the neural network.

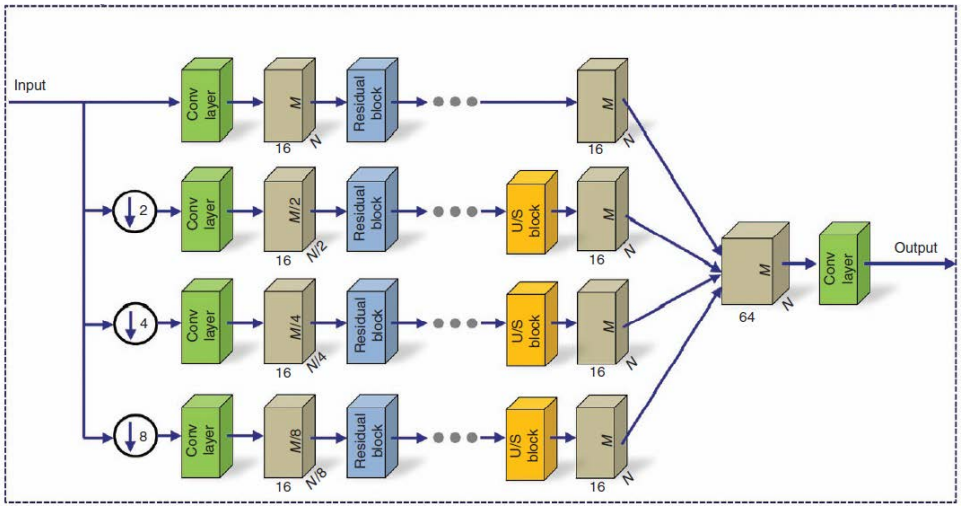

Fig. 2.5: *A network of reconfigurable multi-scale digital holograms.*

2.2.2. Pooled core subsampling. The lower sampling used the largest pool size, a 2x2 pool. Its primary purpose is to reduce the scale of feature mapping, maintain helpful information, increase the perception field, and, to some extent, prevent overfitting and reduce the difficulty of solving the network structure.

2.2.3. Using Nearest Neighbor Padding. The goal is to decode step by step to restore the original image size. After up-sampling the image, the size of the image will be doubled.

2.2.4. Long Jump Connection. This operation connects the feature graph channels of the output of the shallow network and the deep network together, and the result is used as the input of the next layer so that the deeper network can retain useful shallow information while avoiding gradient disappearance and improving network performance [11].

2.2.5. Output convolution layer. This is simply a combination of convolution and activation layers used to produce a single-channel image.

The network structure used in the second experiment is represented in Figure 2.5. The U-Net in this architecture is represented by the dotted boxes in the Figure 2.3 architecture and otherwise has the same functionality as the corresponding modules in the Figure 2.3 architecture [12]. The numbers above the matrix box represent the channels in the current feature graph. One represents the input and the output as grayscale images, and 40, 20, and 20 represent the number of channels. They also indicate that C1 is 40, 20, and 20 in the modified U-Net architecture. There are three levels from top to bottom [13]. The first level is a 256x256 three-dimensional image. Fix the current model parameters when done. A digital holographic image with a size of 512x512 is passed through the two front and back network structures. Only the second network is learned, and then the parameters of the second network are fixed. The three-level network architecture is added so that every network can pass 640x480 digital holographic, while the three-layer network only needs to learn the network parameters [14]. Since the following layer network can use the local characteristic map extracted from the previous layer network, the number of all network parameters can be reduced. This network structure can effectively solve the problem of multiple extractions of the same image, thus reducing the complexity of modeling and realizing the reconstruction of images of different sizes.

2.3. Generation of data sets and network training. Digital holograms are generated when a computer simulates digital holographic imaging. This project intends to scale up to 18,000 handwritten drawings in the MNIST standard library to obtain amplitude information [15]. The 18,000 images of Chinese characters are normalized and multiplied by 1.9π according to A particular proportion, that is, the wavelength of the illuminated object is $\eta = 632.8$ nm, the distance between the illuminated object and the recording surface of

Table 3.1: Simulation Environment Settings.

Name	Settings
CPU	Intel265GHz4 core
RAM	16G
SDD	500
OS	Win10PersonalEdition

the hologram is $s = 0.3086m$, and the size of the recording surface of the hologram is 5 mm. The reference light is parallel. The Angle of reference light with the x-axis and the Y-axis is set as $\pi/2.02$ and $\pi/2$, and the sampling quantity is $256 \times 256, 512 \times 512, 640 \times 480$. The complex amplitude distribution of object wave on the digital holographic plane is obtained by formula (1), and then it coherently overlaps with the reference wave to obtain 6000 digital holograms of different sizes. Five thousand cases were selected as training and 1000 as test samples [16]. The training loss function uses the mean square error loss function, which represents the sum of squares of errors at the corresponding points of the predicted and original data. The expression is

$$\text{lose}_{MSE} = \frac{1}{n}\sum_{i=1}^{n}(v_i - \bar{v}_i)^2$$

n represents the size of the photo. v_i represents the amplitude information or the i value of the phase information after reconstruction; $\bar{v}_i$ represents i values associated with the initial data [17]. The weights are optimized by the Adam optimization method. Measures were taken to end the training session early when mistakes were made to avoid over-learning. A deep neural network learning framework based on NvidiaRTX2080Ti is constructed by using Pytorch technology.

3. Case analysis.

3.1. Environment Settings. This project intends to use a convolutional neural network and BP neural network for detection [18]. The above algorithms are compared under the experimental conditions given in Table 3.1.

3.2. Experimental object of image reconstruction in laser holography. Five typical three-dimensional images are selected for experiments to verify the universality of the algorithm [19]. Fifty images were selected as simulation tests for different types of laser holograms. The representative image is shown in Figure 3.1.

3.3. Study on image reconstruction in laser holography. The reconstruction results of various stereo images obtained by the three measurement methods are compared, and the results are shown in Figure 3.2. The results show that the accuracy of laser hologram image reconstruction based on deep learning neural networks is better than 95%. The advantages of laser holographic image reconstruction based on deep learning neural network theory are proven.

3.4. Comparison of image reconstruction effects of laser holography. The reconstruction speed in existing large three-dimensional images is also a significant problem. According to the analysis of Figure 3.3, it can be seen that the reconstruction of the 3D stereo image reconstructed by the neural network method based on deep learning takes about 20 milliseconds, the 3D reconstruction based on the BP network takes about 30 milliseconds, and the reconstruction of the convolutional neural network takes about 35 milliseconds.

4. Conclusion. A new idea of three-dimensional image reconstruction using a deep neural network is studied. Its main objective is to improve image reconstruction accuracy in laser holography. The deep neural network model is applied to the reconstruction of laser holographic images, improving the reconstruction effect of laser holographic images. This will help the processing of laser holograms in the future. This project will open up a new way to improve the image quality of laser holographic image reconstruction.

Fig. 3.1: *Experimental subjects of image reconstruction in laser holographic imaging.*

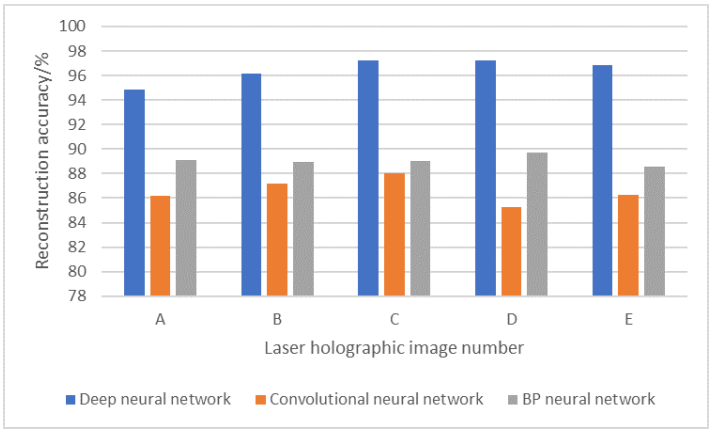

Fig. 3.2: *Image reconstruction accuracy of laser holographic imaging by different methods.*

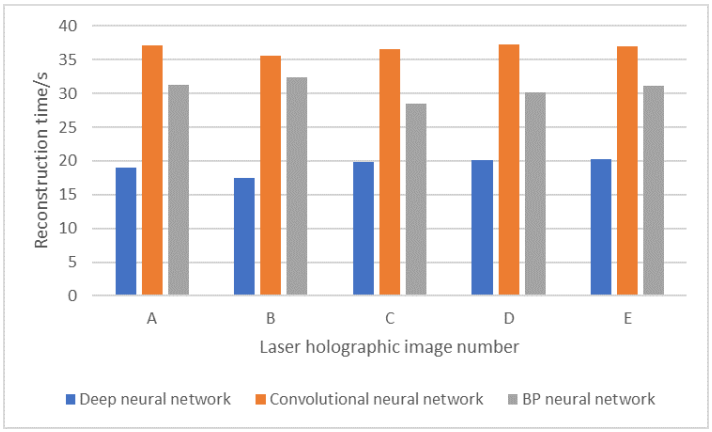

Fig. 3.3: *Image reconstruction time in different ways in laser holography.*

Acknowledgements. The work was supported by Weinan Science and Technology Bureau (WXQY002-011).

REFERENCES

[1] Huang, L., Liu, T., Yang, X., Luo, Y., Rivenson, Y., & Ozcan, A. (2021). Holographic image reconstruction with phase recovery and autofocusing using recurrent neural networks. ACS Photonics, 8(6), 1763-1774.
[2] Melanthota, S. K., Gopal, D., Chakrabarti, S., Kashyap, A. A., Radhakrishnan, R., & Mazumder, N. (2022). Deep learning-based image processing in optical microscopy. Biophysical Reviews, 14(2), 463-481.
[3] Shi, L., Li, B., Kim, C., Kellnhofer, P., & Matusik, W. (2021). Towards real-time photorealistic 3D holography with deep neural networks. Nature, 591(7849), 234-239.
[4] Pirone, D., Sirico, D., Miccio, L., Bianco, V., Mugnano, M., Ferraro, P., & Memmolo, P. (2022). Speeding up reconstruction of 3D tomograms in holographic flow cytometry via deep learning. Lab on a Chip, 22(4), 793-804.
[5] Zeng, T., Zhu, Y., & Lam, E. Y. (2021). Deep learning for digital holography: a review. Optics Express, 29(24), 40572-40593.
[6] Rekola H, Berdin A, Fedele C, et al. (2020). Digital holographic microscopy for real-time observation of surface-relief grating formation on azobenzene-containing films. Scientific Reports, 10(1), 19642.
[7] Lee, M. H., Lew, H. M., Youn, S., Kim, T., & Hwang, J. Y. (2022). Deep learning-based framework for fast and accurate acoustic hologram generation. IEEE Transactions on Ultrasonics, Ferroelectrics, and Frequency Control, 69(12), 3353-3366.
[8] Rahmani, B., Oguz, I., Tegin, U., Hsieh, J. L., Psaltis, D., & Moser, C. (2022). Learning to image and compute with multimode optical fibers. Nanophotonics, 11(6), 1071-1082.
[9] Kim, W., Park, B. S., Kim, J. K., Oh, K. J., Kim, J. W., Kim, D. W., & Seo, Y. H. (2020). Deep learning-based super resolution for phase-only holograms. Journal of Broadcast Engineering, 25(6), 935-943.
[10] Gao, P., & Yuan, C. (2022). Resolution enhancement of digital holographic microscopy via synthetic aperture: a review. Light: Advanced Manufacturing, 3(1), 105-120.
[11] MacNeil, L., Missan, S., Luo, J., Trappenberg, T., & LaRoche, J. (2021). Plankton classification with high-throughput submersible holographic microscopy and transfer learning. BMC Ecology and Evolution, 21(1), 1-11.
[12] Potter, C. J., Hu, Y., Xiong, Z., Wang, J., & McLeod, E. (2022). Point-of-care SARS-CoV-2 sensing using lens-free imaging and a deep learning-assisted quantitative agglutination assay. Lab on a Chip, 22(19), 3744-3754.
[13] Sun, J., Tárnok, A., & Su, X. (2020). Deep learning-based single-cell optical image studies. Cytometry Part A, 97(3), 226-240.
[14] Huang, L., Chen, H., Liu, T., & Ozcan, A. (2023). Self-supervised learning of hologram reconstruction using physics consistency. Nature Machine Intelligence, 5(8), 895-907.
[15] Sakib Rahman, M. S., & Ozcan, A. (2021). Computer-free, all-optical reconstruction of holograms using diffractive networks. ACS Photonics, 8(11), 3375-3384.
[16] Xu, G., Jin, B., Yang, S., & Liu, P. (2023). Field recovery from digital inline holographic images of composite propellant combustion base on denoising diffusion model. Optics Express, 31(23), 38216-38227.
[17] ONUR, T. Ö., & KAYA, G. U. (2022). Application of Binary Genetic Algorithm for Holographic Vascular Mimicking Phantom Reconstruction. Balkan Journal of Electrical and Computer Engineering, 10(1), 16-22.
[18] Kang, I., De Cea, M., Xue, J., Li, Z., Barbastathis, G., & Ram, R. J. (2022). Simultaneous spectral recovery and CMOS micro-LED holography with an untrained deep neural network. Optica, 9(10), 1149-1155.
[19] Meng, Z., Pedrini, G., Lv, X., Ma, J., Nie, S., & Yuan, C. (2021). DL-SI-DHM: A deep network generating the high-resolution phase and amplitude images from wide-field images. Optics Express, 29(13), 19247-19261.

Edited by: Zhigao Zheng
Special issue on: Graph Powered Big Aerospace Data Processing
Received: Dec 25, 2023
Accepted: Jan 15, 2024